Received June 2002
Revised November 2002
Accepted December 2002

Effect of space ratio and corrugation angle on convection enhancement in wavy channels

G. Comini, C. Nonino and S. Savino
Dipartimento di Energetica e Macchine, Università degli Studi di Udine, Via delle Scienze, Udine, Italy

Keywords *Convection, Channels, Finite elements*

Abstract *By neglecting the influence of tubes, this paper adopts a simplified two-dimensional approach to deal with laminar convection of air through wavy finned-tube exchangers. Pressure drop and heat transfer characteristics are investigated in the fully developed region of the flow channels between adjacent fins. The solutions are presented for several space ratios (height over length of a module) and two corrugation angles. They concern laminar flows both below and above the onset of the self-sustained oscillations that precede the transition to turbulence. Fully developed velocity and thermal fields are computed by imposing anti-periodic conditions at inlet/outlet sections of a single calculation cell. In the range of Reynolds numbers investigated, Nusselt numbers and friction factors first increase with space ratios (up to a value depending on the corrugation angle), then start decreasing with increasing space ratios.*

Nomenclature

a = thermal diffusivity
A = peak-to-peak amplitudes of time oscillations of the Nusselt number
D_h = hydraulic diameter
f = friction factor
h = convection heat transfer coefficient
H = height
j = Colburn factor for heat transfer
L = length of a corrugation module
Nu = Nusselt number
p = pressure
$\tilde{p}$ = periodic component of pressure
Pr = Prandtl number
q = heat flow rate
Re = Reynolds number
S = area of the exchange surface
St = Strouhal number
t = temperature
u,v = velocity components in the (x,y) directions
x,y = Cartesian coordinates
y' = distance from the lower boundary in the y direction
α = overall pressure gradient in the flow direction
β = corrugation angle
ν = kinematic viscosity
ϑ = time
θ = dimensionless time
Θ = period

Subscripts

b = bulk
i = inflow
lm = logarithmic mean
o = outflow
w = wall

Superscripts

$\bar{}$ = space-averaged value

International Journal of Numerical Methods for Heat & Fluid Flow
Vol. 13 No. 4, 2003
pp. 500-519

0961-5539
DOI 10.1108/09615530310475939

Introduction

To reduce the airside thermal resistance in compact heat exchangers, recourse is usually made to extended surfaces in the form of fins. This way the exchange area can be considerably increased. In modern applications, however, also convection coefficients must be augmented since, to limit noise emissions, frontal air velocities are maintained low and the resulting flows are in the laminar, or transitional range. Among the surfaces that present convection enhancing irregularities, wavy fins have been frequently employed in the past for their simplicity, and are still preferred today in many low-cost applications. By simplifying the actual flow in a tube-fin exchanger to a channel flow between parallel fins, we neglect the presence of tubes. However, we can still adequately model the flow in the passages between adjacent wavy fins, and make significant comparisons with the flow in the corresponding passages between adjacent plain fins.

Forced convection in wavy channels has been extensively studied in the past as illustrated, for example, in the review by Ergin *et al.* (2001). Here we present a critical discussion of the studies which are most relevant to this paper. Pioneering work on wavy channels was carried out by Goldstein and Sparrow (1977). They used the naphtalene sublimation technique to determine convection coefficients in a short domain consisting of only two corrugation cycles. The corrugation angle β was equal to 21° and the space ratio, height H over length of a corrugation cycle L, was equal to 0.178. It was found that flow separations on the peaks of the corrugations caused a decrease in the local heat transfer rates, while relatively large increases were evidenced in the reattachment regions. The global effect was neutral, at least for low Reynolds number flows.

A few years later, using water as the working fluid, O'Brien and Sparrow (1982) and Sparrow and Comb (1983) determined convection coefficients and friction factors in a channel with ten corrugation cycles and a corrugation angle $\beta = 30°$. The height of the channel was changed in order to obtain two values of the space ratio ($H/L = 0.419$ and $H/L = 0.289$). In the turbulent flow regime investigated ($1{,}500 \leq \mathrm{Re} \leq 25{,}000$), both friction factors and convection coefficients were significantly enhanced with respect to a parallel-plate channel. In particular, the increase in the space ratio gave rise to a 30 per cent increase in the fully developed Nusselt number, but the friction factor more than doubled. Thus performance differences between the two channels (with identical pumping power, pressure gradient, or mass flow), were not sufficiently great to indicate a clear superiority of one over the other.

The effect of the space ratio on heat transfer and pressure drop was investigated also by Molki and Yuen (1986) for $4{,}000 \leq \mathrm{Re} \leq 35{,}000$, in both the developing and the fully developed flow regions. The angle of corrugation was 30° and the best thermal performance, with identical pressure loss, was achieved when the space ratio was the largest ($H/L = 0.5$).

Ali and Ramadhyani (1992) measured heat transfer and pressure drop, under developing flow conditions, in a channel with five corrugation cycles and a corrugation angle $\beta = 20°$. They used two values of the cannel height yielding two different values of the space ratio ($H/L = 0.23$ and $H/L = 0.15$). Their attention was directed to the laminar and transitional regimes, and heat transfer data were obtained over the range $100 \leq \mathrm{Re} \leq 4{,}000$. In the steady laminar range, convection enhancements were marginal with respect to a parallel-plate channel, but friction factors were significantly greater in wavy channels. Once again the best thermal performance (with identical pumping power, pressure gradient, or mass flow) was achieved when the space ratio was the largest ($H/L = 0.23$).

Using steady flow models Asako *et al.* (1988), Xin and Tao (1988), and Yang *et al.* (1997) studied flow and heat transfer in the fully developed region of two-dimensional channels for several space ratios and corrugation angles. Xin and Tao (1988) and Asako *et al.* (1988) employed finite difference methods and considered the laminar flow range ($100 \leq \mathrm{Re} \leq 1{,}000$), while Yang *et al.* (1997) utilised a finite volume method and considered both the laminar and the transitional flow range ($100 \leq \mathrm{Re} \leq 2{,}500$). They all found that convection was enhanced by increasing corrugation angles and increasing space ratios. They also found that Nusselt numbers increased with the Reynolds number, despite the steady models adopted. These latter findings, however, do not agree with the conclusions reached by Fiebig (1996), who performed numerical simulations on the same geometries and claimed that no remarkable enhancement of convection occurred in two-dimensional wavy channels as long as the flow remained steady.

By means of an unsteady flow model and a finite element method, Comini *et al.* (2002) determined convective coefficients and friction factors, for $100 \leq \mathrm{Re} \leq 1{,}000$, in a two-dimensional channel with a space ratio $H/L = 0.22$ and a corrugation angle $\beta = 20°$. In the steady laminar range, convection coefficients were larger in the entrance region than in the fully developed region. In the fully developed region, below the critical value of the Reynolds number, convection enhancements were marginal with respect to a parallel-plate channel, even if friction factors raised significantly. With increasing Reynolds numbers, the onset of time-periodic flow oscillations occurred first in the fully developed region, and then moved upstream into the entrance region. Flow oscillations, associated with transverse vortices, enhanced convection by transporting fluid particles from the walls to the core and downstream. On the contrary, transverse vortices that remained steady only increased friction factors by creating recirculation zones where no fresh fluid entered.

The aforementioned studies represent a substantial base of data. In particular, all studies seem to agree on the enhancement effects connected with the increase of the space ratio H/L and/or the corrugation angle β (at least above the critical value of the Reynolds number). However, very few

experimental studies refer to low Reynolds number flows, and no experimental study takes into proper account the effect of the space ratio. In fact, changing systematically the geometry of an experimental apparatus is a very expensive task. Conversely, most numerical investigations have been based on the assumption of steady flows and, consequently, cannot model the shedding of transverse vortices. The aim of the present paper is to fill the gaps left by previous investigations, using a finite element approach that accounts for the time dependent physics of the flow. The model utilized here has been proposed by Nonino and Comini (1998), and has been used also by Comini *et al.* (2002) for the fully developed regions of wavy channels. In the present study, we investigate the effects of space ratios and corrugation angles on fully developed convection of air (Pr = 0.7) in wavy channels. Flows are always laminar, both below and above the critical value of the Reynolds number corresponding to the onset of vortex shedding processes.

Statement of the problem

According to the two-dimensional approach illustrated by Comini *et al.* (2002), a typical tube-fin exchanger can be schematised by a series of identical geometrical modules such as the one shown in Figure 1(a). In this paper we consider several space ratios *H/L* in the range from 0.1 to 0.45, and two values of the corrugation angle: $\beta = 20°$ and 30°.

After a short distance from the entrance the velocity and thermal fields repeat themselves, from module to module, attaining a fully developed character. In the fully developed region, the repetitive fields allow the limitation of the analysis to a single module, such as the one enclosed by the periodic

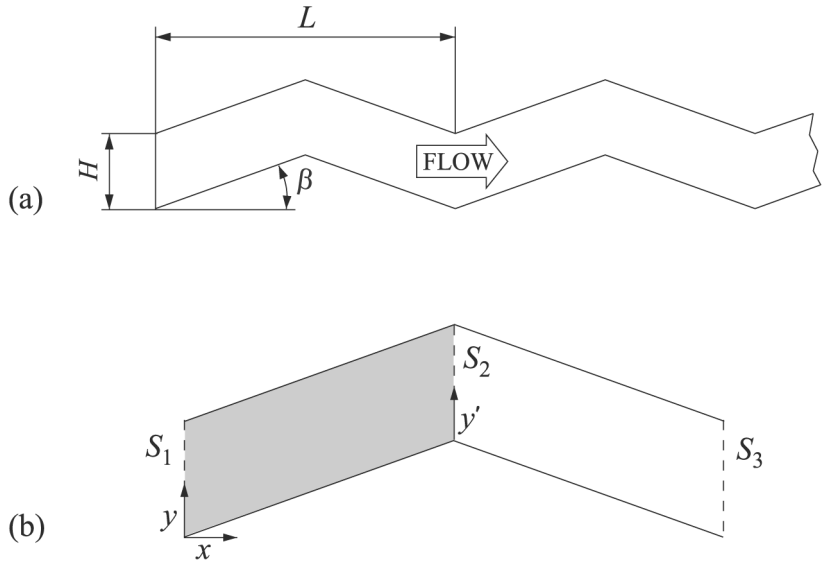

Figure 1.
Flow and convective heat transfer in wavy channels: (a) schematic representation of the geometry and (b) computational cell in the fully developed region

boundaries S_1 and S_3 in Figure 1(b). In the present case, however, it is possible to reduce the computational domain still further. With reference to Figure 1(b), in fact, one can consider only a single half-module, such as the one enclosed by the anti-periodic boundaries S_1 and S_2. On these anti-periodic boundaries, normal velocity components at corresponding points have the same value and the same sign, while tangential velocity components have the same absolute value but opposite sign. The relationships between dimensionless temperature distributions on S_1 and S_2 can be found, following the procedure illustrated by Nonino and Comini (1998), and Comini *et al.* (2002).

The flow field

Under the above assumptions, the momentum and continuity equations governing the laminar flow of air can be written as

$$\frac{\partial u}{\partial \vartheta} + u\frac{\partial u}{\partial x} + v\frac{\partial u}{\partial y} = \nu\left(\frac{\partial^2 u}{\partial x^2} + \frac{\partial^2 u}{\partial y^2}\right) - \frac{1}{\rho}\frac{\partial p}{\partial x} \tag{1}$$

$$\frac{\partial v}{\partial \vartheta} + u\frac{\partial v}{\partial x} + v\frac{\partial v}{\partial y} = \nu\left(\frac{\partial^2 v}{\partial x^2} + \frac{\partial^2 v}{\partial y^2}\right) - \frac{1}{\rho}\frac{\partial p}{\partial y} \tag{2}$$

$$\frac{\partial u}{\partial x} + \frac{\partial v}{\partial y} = 0 \tag{3}$$

In the fully developed flow region, the average pressure gradient is constant in the axial direction. Consequently, with reference to the situation shown in Figure 1(b), we can write

$$p(x, y) = -\alpha x + \tilde{p}(x, y) \tag{4}$$

as suggested by Patankar *et al.* (1977). In the above equation, α is a constant representing the average pressure gradient in the main flow direction x, while $\tilde{p}$ is the periodic component of pressure.

On the basis of equation (4) the momentum equations, governing the fully developed laminar flow of air, can be modified as follows

$$\frac{\partial u}{\partial \vartheta} + u\frac{\partial u}{\partial x} + v\frac{\partial u}{\partial y} = \nu\left(\frac{\partial^2 u}{\partial x^2} + \frac{\partial^2 u}{\partial y^2}\right) + \frac{1}{\rho}\left(\alpha - \frac{\partial \tilde{p}}{\partial x}\right) \tag{5}$$

$$\frac{\partial v}{\partial \vartheta} + u\frac{\partial v}{\partial x} + v\frac{\partial v}{\partial y} = \nu\left(\frac{\partial^2 v}{\partial x^2} + \frac{\partial^2 v}{\partial y^2}\right) - \frac{1}{\rho}\frac{\partial \tilde{p}}{\partial y} \tag{6}$$

Appropriate conditions must be imposed on wall, anti-periodic, inflow and outflow boundaries. On wall boundaries, the usual no-slip boundary condition

$$u = v = 0 \tag{7}$$

is adopted.

The anti-symmetric periodicity between boundaries S_1 and S_2 yields the conditions

$$\tilde{p}(L/2, H - y') = \tilde{p}(0, y) \tag{8}$$

$$u(L/2, H - y') = u(0, y) \tag{9}$$

$$v(L/2, H - y') = -v(0, y) \tag{10}$$

where y' is the distance from the lower boundary measured in the y direction, H is the height, and L is the projected length of one module. In fully developed periodic flows, conditions (9) and (10) do not involve the specification of any inflow velocity. Therefore, the pressure gradient α must be adjusted iteratively, as described by Nonino and Comini (1998), until the desired value of the average "inflow" velocity $\bar{u}$ is reached.

The behaviour of the flow is determined by the Reynolds number

$$\mathrm{Re} = \frac{\rho \bar{u} D_\mathrm{h}}{\mu} = \frac{2\rho \bar{u} H}{\mu} = \frac{2\dot{m}}{\mu} \tag{11}$$

where $D_\mathrm{h} = 2H$ is the hydraulic diameter. The pressure drop depends on the Reynolds number and the apparent friction factor can be expressed as

$$f = \frac{\alpha D_\mathrm{h}}{\rho \bar{u}^2/2} \tag{12}$$

since it is directly related to the average pressure gradient α.

The temperature field

In the absence of volumetric heating, and neglecting the effects of viscous dissipation, the two-dimensional energy equation can be written as

$$\frac{\partial t}{\partial \vartheta} + u\frac{\partial t}{\partial x} + v\frac{\partial t}{\partial y} = a\left(\frac{\partial^2 t}{\partial x^2} + \frac{\partial^2 t}{\partial y^2}\right) \tag{13}$$

where a is the thermal diffusivity.

Appropriate conditions must be imposed on wall, anti-periodic, inflow and outflow boundaries. On top and bottom walls, we specify the same wall temperature

$$t = t_\mathrm{w} \tag{14}$$

For anti-periodic boundaries S_1 and S_2 in the fully developed flow region, we cannot write any simple relationship. However, as suggested by Kelkar and Patankar (1987) and illustrated by Nonino and Comini (1998), we can use the following equation

$$\frac{t(L/2, H - y') - t_w}{t_b(L/2) - t_w} = \frac{t(0, y) - t_w}{t_b(0) - t_w} \tag{15}$$

which leads to the condition

$$t(L/2, H - y') = \left[1 + \frac{t_b(L/2) - t_b(0)}{t_b(0) - t_w}\right] t(0, y) - \frac{t_b(L/2) - t_b(0)}{t_b(0) - t_w} t_w \tag{16}$$

In the above equations t_b is the bulk temperature, which can be conveniently defined as

$$t_b = \frac{\int_0^H |u| t \, dy}{\int_0^H |u| \, dy} \tag{17}$$

Equation (16) contains two unknown quantities: the bulk temperature at inflow $t_b(0)$ and the difference between the bulk temperatures at outflow and inflow. Thus, in the solution process, we first impose the value of the bulk temperature difference, and then iterate until convergence is reached for a value of $t_b(0)$ which verifies the periodicity condition.

The Reynolds number and the Prandtl number $\mathrm{Pr} = \nu/a$ determine the behaviour of the temperature field. This behaviour is characterized by the overall, i.e. space-averaged, Nusselt number, defined as

$$\mathrm{Nu} = \frac{\bar{h} D_h}{k} = \frac{2\bar{h} H}{k} \tag{18}$$

In the above equation, the average heat transfer coefficient is defined as

$$\bar{h} = \frac{q}{S \Delta t_{lm}} \tag{19}$$

on the basis of the absolute value q of the heat transfer rate, the exchange area S, and the log-mean temperature difference

$$\Delta t_{lm} = \frac{[t_w - t_b(L/2)] - [t_w - t_b(0)]}{\ln\{[t_w - t_b(L/2)]/[t_w - t_b(0)]\}} \tag{20}$$

computed over a half-module.

Numerical solution

The momentum, continuity and energy equations are solved by an equal-order, finite-element procedure based on the projection algorithm illustrated by Nonino and Comini (1997) and Nonino *et al.* (1999). At each time step, a pseudovelocity field is obtained by neglecting the pressure gradients in the momentum equations. Then, by enforcing continuity on the pseudo-velocity

field, a tentative pressure is estimated and the momentum equations are solved for the tentative velocity field. Afterwards, continuity is enforced again to find pressure corrections. Pressure corrections are also used to find the velocity corrections that project the tentative velocity field onto a divergence-free space. Once the velocity field has been found, the energy equation is solved before moving to the next step.

The momentum and energy equations are dealt with as particular versions of a general transport equation, written in the time-discretized form

$$\gamma\frac{\phi^{n+1}-\phi^{n}}{\Delta\vartheta}+\gamma v^{n}\cdot[\tau_{v}\nabla\phi^{n+1}+(1-\tau_{v})\nabla\phi^{n}]$$
$$=\Gamma[\tau_{\Gamma}\nabla^{2}\phi^{n+1}+(1-\tau_{\Gamma})\nabla^{2}\phi^{n}]+\dot{s} \quad (21)$$

for a generic variable ϕ. The properties γ and Γ, and the volumetric source rate $\dot{s}$ are identified by inspection of the appropriate original equations for velocity components, pressure and temperature. The weighting factors τ_v and τ_Γ, both in the range from 0 to 1, allow the selection of different time-integration schemes. For example the Crank-Nicolson scheme, used in this work, results from the choice: $\tau_v = \tau_\Gamma = 0.5$. The pressure equation and the pressure correction equation are particular versions of the Poisson equation, which can be obtained from equation (21) by assuming $\gamma = 0$ and $\tau_\Gamma = \Gamma = 1$. The space discretization of equation (21) is based on the Bubnov-Galerkin method, which avoids the numerical diffusion connected with upwinding procedures. The periodic boundary conditions are introduced as illustrated in detail by Nonino and Comini (2002) and Comini *et al.* (2002).

In the numerical simulations, the systems of linear equations, arising at each time step from the discretization process, were solved by means of iterative algorithms. The conjugate gradient squared (CGS) method, described by Howard *et al.* (1990), has been used to solve the discretized momentum and energy equations. The modified conjugate gradient method (MCG), illustrated by Gambolati (1988) has been used to solve the symmetric systems obtained from the discretization of the Poisson equations. In both cases, preconditioned matrices have been obtained from an incomplete LU decomposition (ILU).

Results and discussion

The following examples concern the Prandtl number $\mathrm{Pr} = 0.7$ and several Reynolds number in the range $100 \leq \mathrm{Re} \leq 800$. Space ratio values $H/L =$ 0.10, 0.15, 0.20, 0.25 and 0.30 were considered with $\beta = 20°$, while values $H/L = 0.10$, 0.15, 0.20, 0.25, 0.30, 0.35 and 0.45 were considered with $\beta = 30°$. In the computations, we utilized the boundary conditions discussed in the previous sections. The program had already been validated by Comini *et al.* (2002), Nonino and Comini (1998). In particular, by imposing periodicity conditions on a portion of a plain channel, they found that results for the fully

developed situation are independent, as expected, of the Reynolds and Prandtl number. In fact, the numerical results agree, to the third digit, with the analytical solutions: $Nu_0 = 7.5407$ and $(f\,Re)_0 = 96.00$ reported by Shah and Bhatti (1987).

Grid independence was established on the basis of calculations in which the distance between grid points was progressively reduced by 30 per cent from one simulation to another. When a further decrease led to a change in the average Nusselt numbers smaller that 1 per cent, the results were considered grid-independent. In the final simulations we used grids consisting of a minimum of 1,925 nodes, for the largest space ratios, to a maximum of 5,825 nodes, for the smallest space ratios. As usual, grid spacing was finer near the walls. Similarly, time-step independence was established on the basis of preliminary calculations in which the dimensionless time step $\bar{u}\Delta\vartheta/L$ was progressively reduced by 30 per cent from one simulation to another. When a further decrease led to a change in the average Nusselt numbers smaller than 1 per cent, the results were considered independent on the time step. In the final simulations, the backward Euler scheme was used for steady state flows, with a dimensionless value of the time step equal to 0.05, while the Crank-Nicolson scheme was used for time-periodic flows, with a dimensionless value of the time step equal to 0.01.

In the range of Reynolds number investigated, solutions were steady up to the critical values of the Reynolds number Re_{cr}, and became time-periodic for $Re > Re_{cr}$. In time-periodic situations, overall parameters were further averaged over a period Θ, yielding single representative values. This way time averaged values

$$\langle\varphi\rangle = \frac{1}{\Theta}\int_{\vartheta}^{\vartheta+\Theta} \varphi(\vartheta)\,\mathrm{d}\vartheta \tag{22}$$

were obtained for $\varphi = f$ or Nu. However, to reduce confusion in the notation, the symbol $\langle\ \rangle$ has been omitted in the following.

Influence of geometry

The influence of geometries is best established with reference to steady flows in the sub-critical range. At $Re = 200$ we have such flows in all the channels considered. The corresponding streamline contours are shown in Figure 2. As we can see, the transverse vortices, generated at the peaks of the corrugations, are associated with repeated separations and reattachments of the flow. The irregularities of the flow increase with both the space ratio and the corrugation angle even if, as already pointed out, the flow remains steady. It is also apparent that the irregularities of the flow do not lead to a significant mixing between core and wall regions. Thus it can be expected that, with increasing values of the space ratio and the corrugation angle, friction factors grow but

Nusselt numbers are not significantly enhanced, at least as long as flows remain steady.

Influence of flow oscillations

At Reynolds numbers above the critical value Re_{cr}, the transverse vortices start detaching periodically and moving downstream, leading to a time-periodic behaviour of both velocity and temperature fields. The exact determination of Re_{cr} is an almost impossible task since the transients become longer and the amplitudes of oscillations tend to zero when the critical point is approached. Therefore, the values reported in Table I are slightly above the critical ones, and have been found by a trial-and-error procedure in which temperature oscillations are monitored at selected points. It is interesting to note that Re_{cr} first decreases and then increases with the space ratio. In fact, with decreasing values of the space ratio the behaviour of the flow in wavy channels tends to the behaviour of the flow in a plain channel, since the length of a single module tends to infinity. Similarly, with increasing values of the space ratio, and a constant value of the corrugation angle, the behaviour of the flow tends to the behaviour of the flow in a plain, albeit rough, channel, since the length of a single module tends to zero.

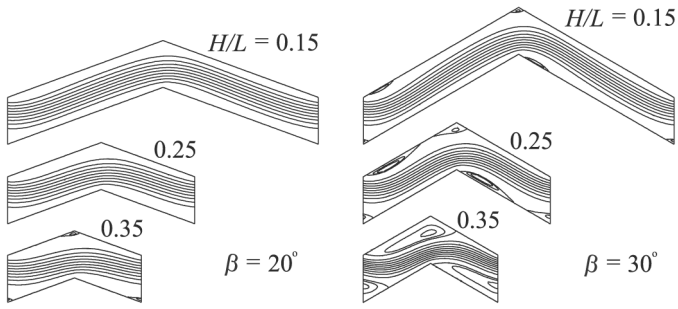

Figure 2.
Streamline contours for steady flows at Re = 200 in wavy channels with space ratios $H/L = 0.15$, 0.25 and 0.35, and corrugation angles $\beta = 20°$ (left) and 30° (right)

Space ratio H/L	$\beta = 20°$	$\beta = 30°$
0.10	690	460
0.15	510	340
0.20	380	220
0.25	360	200
0.30	370	190
0.35	540	180
0.45	–	260

Table I.
Approximate values of the critical Reynolds number in wavy channels

From Table I it can be inferred that, at Re = 700, vortex shedding occurs in all the channels investigated. Thus the streamline contours shown in Figure 3, are instantaneous representations. As already pointed out, the self-sustained oscillations of the flow transport fluid particles from the walls to the core and downstream, significantly enhancing convection.

The behaviour of the Nusselt number, at Re = 700, is shown in Figures 4 and 5 for $\beta = 20°$ and 30°, respectively. In these figures we report, on the left, the variations of the space averaged Nusselt number vs the dimensionless time

$$\theta = \frac{\vartheta \bar{u}}{D_h} \tag{23}$$

and, on the right, the corresponding spectra of the peak-to-peak amplitudes A_{NU} as a function of the Strouhal number

$$St = \frac{D_h}{\bar{u}\Theta} \tag{24}$$

As we can see, both the time behaviour of the Nusselt number and the amplitude of the sub-harmonics depend on the space ratio and the corrugation angles.

Influence of the Reynolds number

The momentum and heat transfer characteristics of wavy channels can be described in terms of overall Nusselt numbers and apparent friction factors multiplied by the Reynolds number. Usually, the Nu and fRe values pertaining to the wavy fins are divided by the corresponding Nu_0 and f_0Re values pertaining to the fully developed region of a plain channel at the same Reynolds number. The behaviours of the ratios f/f_0 and Nu/Nu_0 vs Re are reported in Figures 6 and 7 for $\beta = 20°$ and 30°, respectively. As we can see friction factors always increases with the Reynolds number, while Nusselt numbers increase significantly only above the critical value of the Reynolds number. Furthermore, both friction factors and Nusselt numbers increase when the

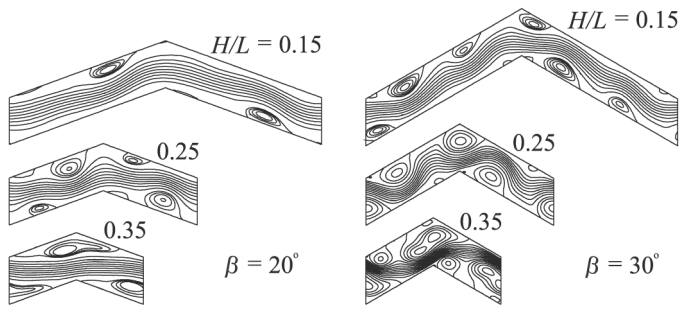

Figure 3.
Instantaneous representations of streamline contours for unsteady flows at Re = 700 in wavy channels with space ratios $H/L = 0.15$, 0.25 and 0.35, and corrugation angles $\beta = 20°$ (left) and 30° (right)

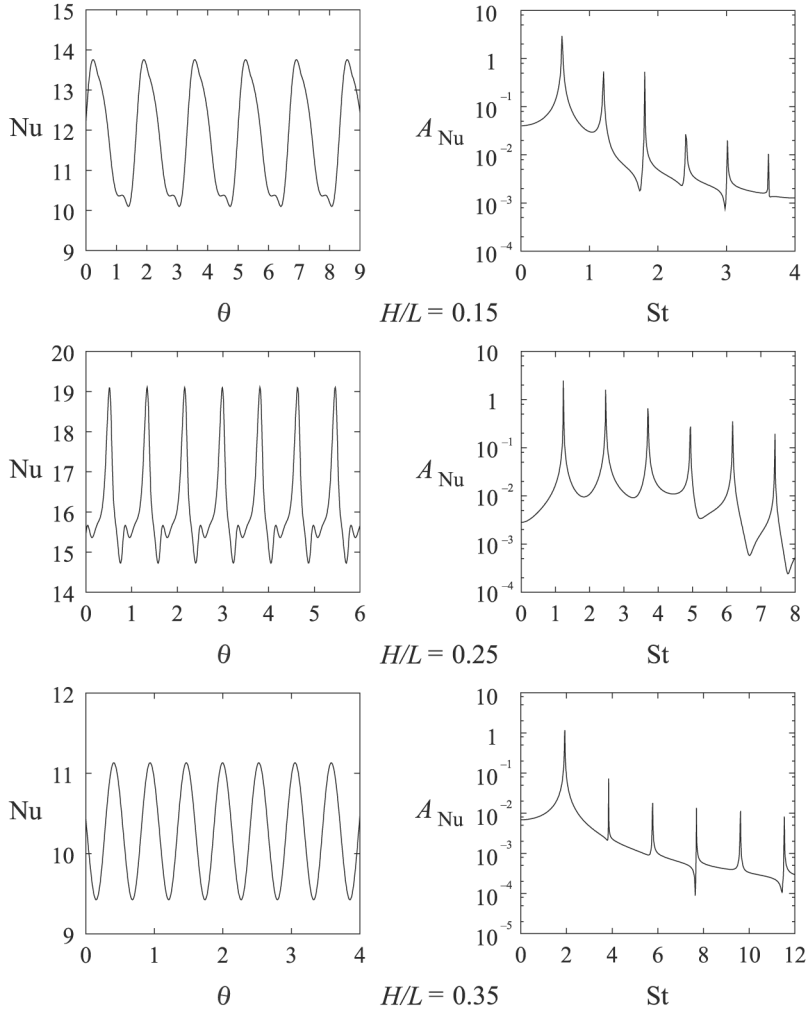

Figure 4.
Unsteady convection at Re = 700 in wavy channels with space ratios $H/L = 0.15$, 0.25 and 0.35, and a corrugation angle $\beta = 20°$: time behaviours of the space-averaged Nusselt number (left) and corresponding spectra (right)

corrugation angle increases from 20° to 30°. On the contrary, with increasing values of the space ratio, the friction factor and the Nusselt number increase but only up to a certain value.

The above findings are better shown in Figure 8 where, for Re = 700, we report the behaviours of the f/f_0 and Nu/Nu_0 ratios vs the space ratio. These results confirm that, with both decreasing and increasing values of the space ratio, the behaviour of the flow in wavy channels tends to the behaviour of the flow in a plain channel. In fact, as already pointed out, the length of a single module tends to infinity with decreasing values of the space ratio, while the flow passage becomes a plain, albeit rough, channel with a constant value of

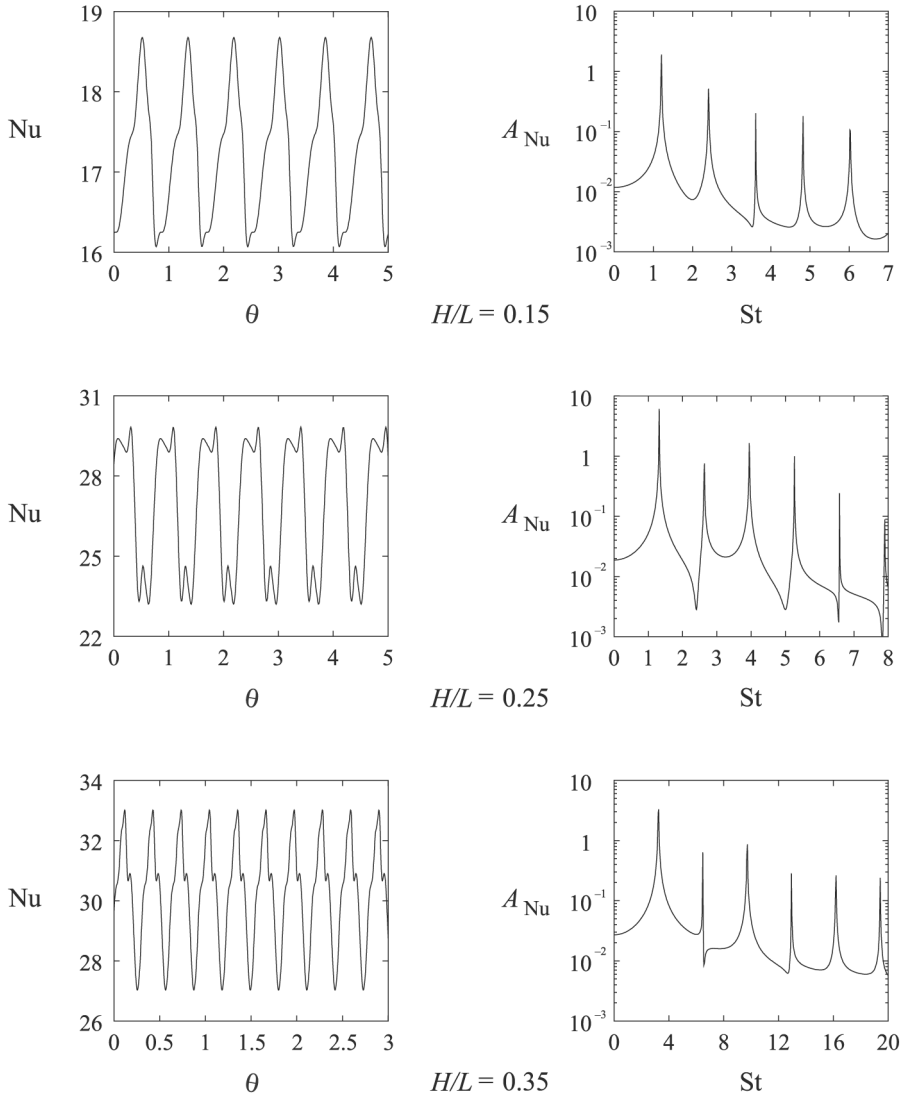

Figure 5.
Unsteady convection at Re = 700 in wavy channels with space ratios $H/L = 0.15$, 0.25 and 0.35, and a corrugation angle $\beta = 30°$: time behaviour of the space-averaged Nusselt numbers (left), and corresponding spectra (right)

the corrugation angle and increasing values of the space ratio. Similar conclusions had been reached by Ergin *et al.* (1996) for the friction factor, and can also be inferred from the numerical results presented by Fiebig (1996) for both the friction factor and the Nusselt numbers.

Evaluation of performances

In boundary layer flows, the momentum and heat transfer characteristics are related by the Chilton-Colburn analogy, which can be written in the form

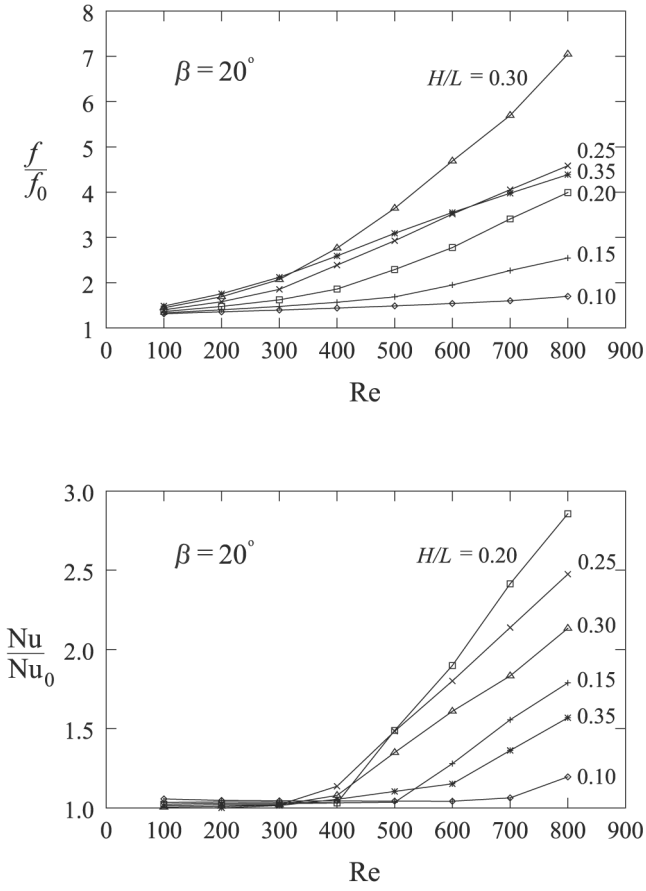

Figure 6.
Apparent friction factors and overall Nusselt numbers vs Reynolds number in wavy channels with different space ratios and a corrugation angle $\beta = 20°$

$$\varepsilon = \frac{j}{f} = \frac{\mathrm{Nu}}{\mathrm{Re}\,\mathrm{Pr}^{1/3}}\frac{1}{f} = \text{const.} \tag{25}$$

where j is the Colburn factor for heat transfer, and ε can be interpreted as a goodness factor. This analogy is strictly valid for boundary layer flows over a flat plate. However, by adjusting the value of the constant, it can be applied with good results to any non-recirculating flow. For example, in the case of $\mathrm{Pr} = 0.7$ and fully developed laminar flow and thermal fields in a plain channel, we obtain

$$\varepsilon_0 = \left(\frac{j}{f}\right)_0 = \frac{\mathrm{Nu}_0}{(f\,\mathrm{Re})_0\mathrm{Pr}^{1/3}} = 0.08847 \tag{26}$$

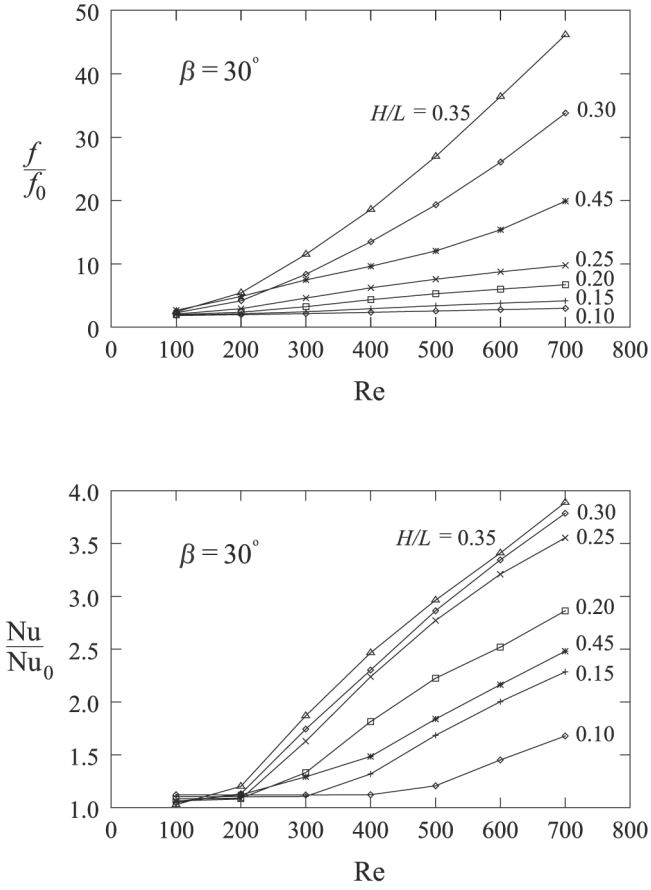

Figure 7.
Apparent friction factors and overall Nusselt numbers vs Reynolds number in wavy channels with different space ratios and a corrugation angle $\beta = 30°$

In recirculating flows, such as the ones occurring in wavy channels, the Chilton-Colburn analogy cannot be expected to hold good. However, the ratio $\varepsilon/\varepsilon_0$ can still be used as a goodness factor in performance comparisons such as the ones shown in Figure 9.

As we can see, the increase in the corrugation angle does not have a beneficial effect in terms of overall performance. Furthermore, the goodness factor reaches a minimum for all configurations just before the onset of the self-sustained oscillations.

Quantitative comparisons

Comparative evaluations of the results obtained are difficult, since the test cases discussed in the literature refer to geometries, flow conditions and fluids that are, almost invariably, different from the ones referred to in this paper. In fact, we have arrived at the comparisons shown in Figure 10 by taking into

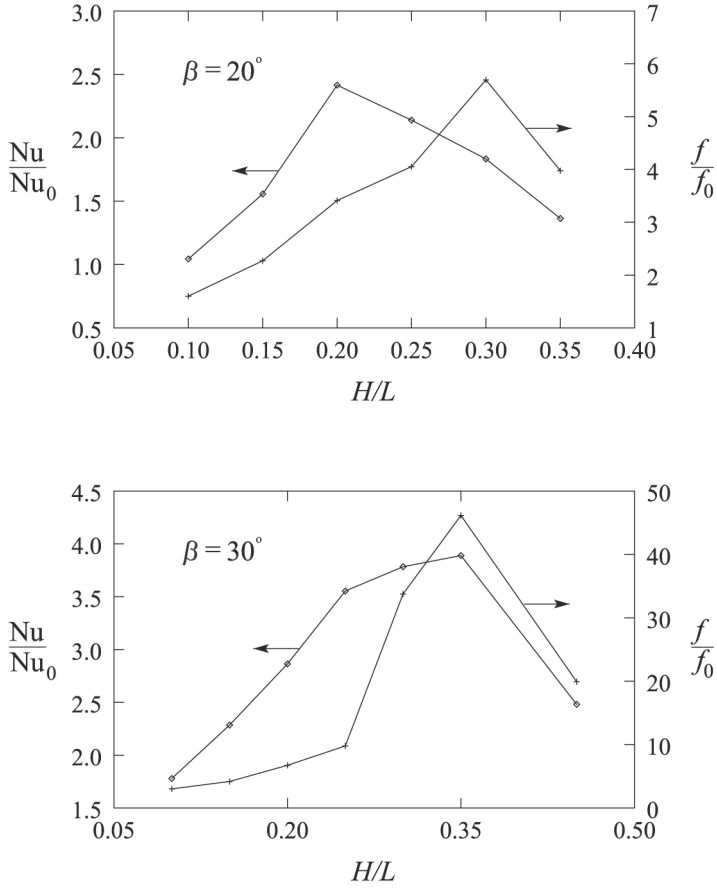

Figure 8.
Apparent friction factors and overall Nusselt numbers vs space ratios at Re = 700, in wavy channels with corrugation angles $\beta = 20°$ (above) and 30° (below)

account literature data for fully developed flows in the $100 \leq \mathrm{Re} \leq 700$ range, and wavy channels which, geometrically, do not differ much from the ones that have been considered in this study.

For the friction factor, literature results that allow a significant comparison have been presented by Ergin *et al.* (2001). They include numerical and experimental data obtained by Asako *et al.* (1989) and Ergin *et al.* (1996, 2001), for the corrugation angle $\beta = 30°$ and the $H/L = 0.43$ and 0.48 space ratios. In Figure 10, the comparison with our results for $\beta = 30°$ and $H/L = 0.45$ shows the expected trend and a reasonably good agreement.

For the Nusselt number, a significant comparison can be established with the numerical results obtained from a steady flow model by Asako *et al.* (1988), for the corrugation angle $\beta = 30°$ and $H/L = 0.14$, 0.29 and 0.42 space ratios. When plotted against the Reynolds number in Figure 10, Asako's data show

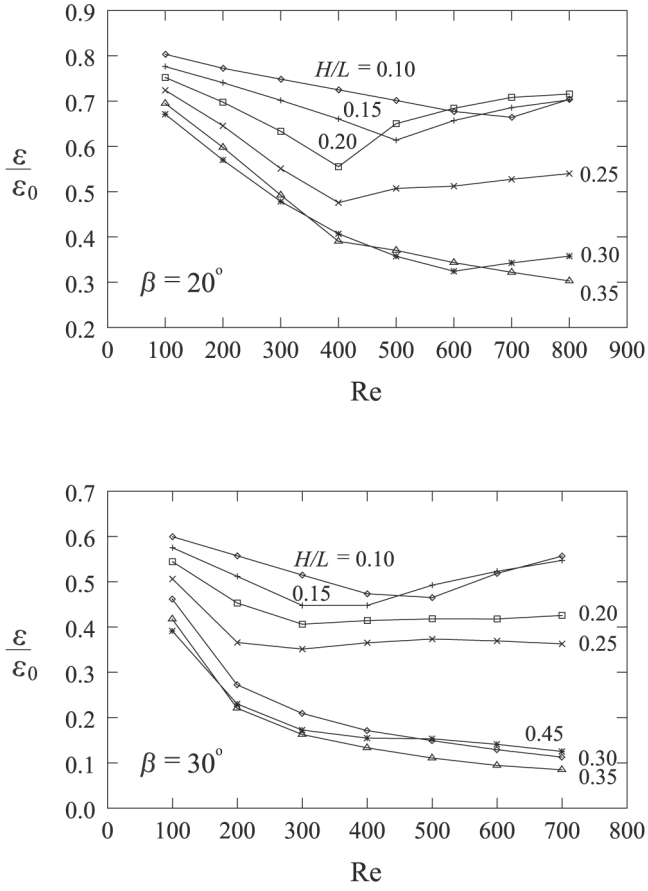

Figure 9.
Goodness factors vs Reynolds numbers in wavy channels with corrugation angles $\beta = 20°$ (above) and 30° (below)

a nearly linear increase of the Nusselt number with the Reynolds number and the aspect ratio. On the contrary, our data for $\beta = 30°$ and $H/L = 0.15$, 0.30 and 0.45 show no remarkable enhancement of convection as long as the flow remains steady. However, these findings are in accordance with Fieblig (1996). The already discussed inversion of the trends with increasing values of the aspect ratio is also apparent in our data.

Conclusions

We have investigated the enhancement of convection in laminar flows of air through wavy finned-tube exchangers. By neglecting the influence of tubes, pressure drop and heat transfer characteristics have been computed in the fully developed regions of wavy flow passages with variable space ratios and corrugation angles. The numerical model adopted is completely general, even

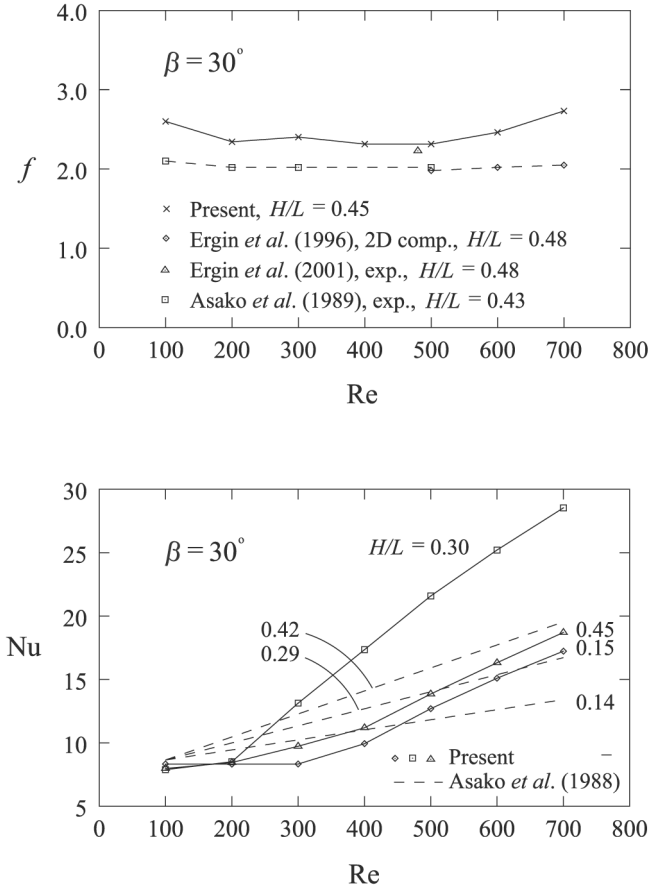

Figure 10.
Comparison of friction factor and Nusselt data for $\beta = 30°$ and different values of the aspect ratio *H/L*

though the discretization process was based on the finite element method. Velocity and temperature fields have been determined first. Quantitative results have then been obtained for apparent friction factors, Nusselt numbers, and goodness factors. In all the situations considered, the fRe parameter of wavy channels is much higher than the one corresponding to the smooth channel. On the contrary, a significant improvement of the average Nusselt number can be obtained only for Reynolds number above the critical value. In this case, the improvement can be attributed to the periodic washing of the channel walls by travelling transverse vortices. Finally, it has been found that both the friction factor and the Nusselt number increase when the corrugation angle β increases from 20° to 30°. On the contrary, with increasing values of the space ratio *H/L*, the friction factor and the Nusselt number increase but only up to a certain value. Consequently, the optimum value of the space ratio depends on both the corrugation angle and the Reynolds number.

References

Ali, M.M. and Ramadhyani, S. (1992), "Experiments on convective heat transfer in corrugated channels", *Experimental Heat Transfer*, Vol. 5, pp. 175-93.

Asako, Y., Nakamura, H. and Faghri, M. (1988), "Heat transfer and pressure drop characteristics in a corrugated duct with rounded corners", *Int. J. Heat Mass Transfer*, Vol. 31, pp. 1237-45.

Asako, Y., Nakamura, H. and Watanabe, S. (1989), "Study of flow in a corrugated duct", *Proc. of the 26th National Heat Transfer Symp. of Japan*, Vol. 1, pp. 31-3 (in Japanese).

Comini, G., Nonino, C. and Savino, S. (2002), "Convective heat and mass transfer in wavy finned-tube exchangers", *International Journal of Numerical Methods for Heat and Fluid Flow*, Vol. 12, pp. 735-55.

Ergin, S., Ota, M. and Yamaguchi, H. (2001), "Numerical study of periodic turbulent flow through a corrugated duct", *Numerical Heat Transfer, Part A*, Vol. 40, pp. 139-56.

Ergin, S., Ota, M., Yamaguchi, H. and Sakamoto, M. (1996), "A numerical study of the effect of interwall spacing on turbulent flow in a corrugated duct", *Proceedings of the ASME Heat Transfer Division, Part 2*, HTD – Vol. 33, pp. 47-54.

Fiebig, M. (1996), "Vortices: tools to influence heat transfer – recent developments", in Celata, G.P., Di Marco, P. and Mariani, A. (Eds), *2nd European Thermal Sciences and 14th UIT National Conference*, ETS, Pisa, Italy, Vol. 1, pp. 41-56.

Gambolati, G. (1988), "*Elements of Numerical Analysis*", Libreria Cortina, Padova, Italy (in Italian).

Goldstein, L. Jr and Sparrow, E.M. (1977), "Heat/mass transfer characteristics for flow in a corrugated wall channel", *J. Heat Transfer*, Vol. 99, pp. 187-95.

Howard, D., Connolley, W.M. and Rollett, J.S. (1990), "Unsymmetric conjugate gradient methods and sparse direct methods in finite element flow simulations", *Int. J. Numer. Meth. Fluids*, Vol. 10, pp. 925-45.

Kelkar, K.M. and Patankar, S.V. (1987), "Numerical prediction of periodically fully developed flow and heat transfer in a parallel plate channel with staggered fins", *J. Heat Transfer*, Vol. 109, pp. 25-30.

Molki, M. and Yuen, C.M. (1986), "Effect of interwall spacing on heat transfer and pressure drop in a corrugated-wall duct", *Int. J. Heat Mass Transfer*, Vol. 29, pp. 987-97.

Nonino, C. and Comini, G. (1997), "An equal order pressure-velocity algorithm for incompressible thermal flows – part 1: formulation", *Numer. Heat Transfer, Part B*, Vol. 32, pp. 1-15.

Nonino, C. and Comini, G. (1998), "Finite-element analysis of convection problems in spatially periodic domains", *Numer. Heat Transfer, Part B*, Vol. 34, pp. 361-78.

Nonino, C. and Comini, G. (2002), "Convective heat transfer in ribbed square channels", *International Journal of Numerical Methods for Heat and Fluid Flow*, Vol. 12, pp. 610-28.

Nonino, C., Comini, G. and Croce, G. (1999), "Three-dimensional flows over backward facing steps", *International Journal of Numerical Methods for Heat and Fluid Flow*, Vol. 9, pp. 224-39.

O'Brien, J.E. and Sparrow, E.M. (1982), "Corrugated-duct heat transfer, pressure drop, and flow visualization", *J. Heat Transfer*, Vol. 104, pp. 410-6.

Patankar, S.V., Liu, C.H. and Sparrow, E.M. (1977), "Fully developed flow and heat transfer in ducts having streamwise-periodic variations of cross-sectional area", *Trans. ASME, J. Heat Transfer*, Vol. 99, pp. 180-6.

Shah, R.K. and Bhatti, M.S. (1987), "Laminar convective heat transfer in ducts", in Kakac, S., Shah, R.S. and Aung, W. (Eds), *Handbook of Single-Phase Convective Heat Transfer*, Chapter 3, Wiley, New York.

Sparrow, E.M. and Comb, J.W. (1983), "Effect of interwall spacing and fluid flow inlet conditions on a corrugated wall heat exchanger", *Int. J. Heat Mass Transfer*, Vol. 26, pp. 993-1005.

Xin, R.C. and Tao, W.Q. (1988), "Numerical prediction of laminar flow and heat transfer in wavy channels of uniform cross-sectional area", *Numer. Heat Transfer*, Vol. 14, pp. 465-81.

Yang, L.C., Asako, Y., Yamaguchi, Y. and Faghri, M. (1997), "Numerical prediction of transitional characteristics of flow and heat transfer in a corrugated duct", *J. Heat Transfer*, Vol. 119, pp. 62-9.